

NUMERICAL SIMULATION OF HYDROTHERMAL CIRCULATION IN THE CASCADE RANGE, NORTH-CENTRAL OREGON

S.E. Ingebritsen and K.M. Paulson

U.S. Geological Survey
Menlo Park, California, U.S.A.

ABSTRACT

Alternate conceptual models to explain near-surface heat-flow observations in the central Oregon Cascade Range involve (1) an extensive mid-crustal magmatic heat source underlying both the Quaternary arc and adjacent older rocks or (2) a narrower deep heat source which is flanked by a relatively shallow conductive heat-flow anomaly caused by regional ground-water flow (the lateral-flow model). Relative to the mid-crustal heat source model, the lateral-flow model suggests a more limited geothermal resource base, but a better-defined exploration target. We simulated ground-water flow and heat transport through two cross sections trending west from the Cascade range crest in order to explore the implications of the two models. The thermal input for the alternate conceptual models was simulated by varying the width and intensity of a basal heat-flow anomaly and, in some cases, by introducing shallower heat sources beneath the Quaternary arc. Near-surface observations in the Breitenbush Hot Springs area are most readily explained in terms of lateral heat transport by regional ground-water flow; however, the deep thermal structure still cannot be uniquely inferred. The sparser thermal data set from the McKenzie River area can be explained either in terms of deep regional ground-water flow or in terms of a conduction-dominated system, with ground-water flow essentially confined to Quaternary rocks and fault zones.

INTRODUCTION

In north-central Oregon a large area of near-zero near-surface conductive heat flow occurs in young (<7 Ma) volcanic rocks of the Cascade Range. In contrast, anomalously high advective and conductive heat discharge has been measured in older (>7 Ma) volcanic rocks at lower elevations. The origin of the anomalously high heat flow observed on the flanks of the Cascade Range in central Oregon is a subject of debate. Blackwell and others (1982) and Blackwell and Steele (1985)

explained the near-surface heat-flow observations in terms of an extensive mid-crustal magmatic heat source underlying both the Quaternary (<2 Ma) arc and adjacent older rocks (Figure 1a). More recently, Blackwell and Baker (1988) and Blackwell and others (1989) have suggested that the thermal effects of hydrothermal circulation may be locally superimposed on the effects of this extensive mid-crustal heat source. An alternate model (Ingebritsen and others, 1989) involves a narrower deep heat source essentially confined to the Quaternary arc, flanked by a relatively shallow conductive heat-flow anomaly caused by regional ground-water flow (Figure 1b).

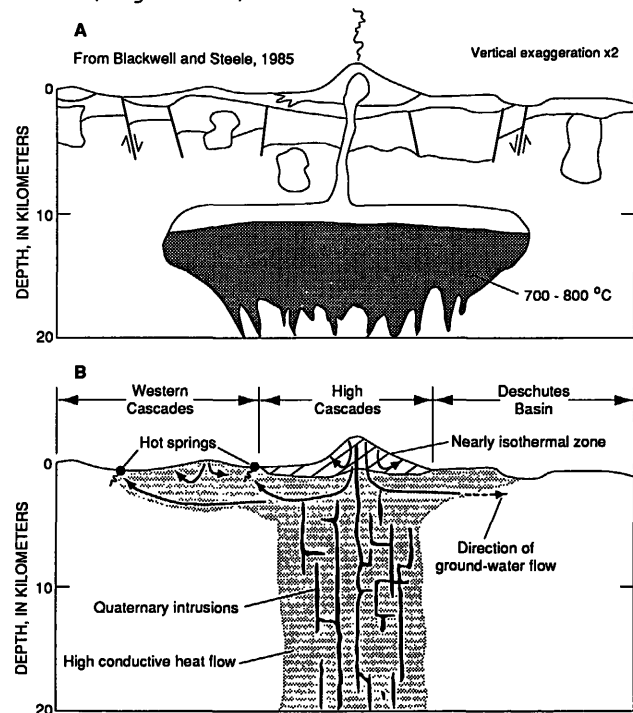


Fig. 1 Conceptual models of the thermal structure of the north-central Oregon Cascades, showing (a) the extensive mid-crustal magmatic heat source proposed in earlier studies (e.g. Blackwell and others, 1982; 1989; Blackwell and Steele, 1985) and (b) the lateral-flow model, with magmatic heat sources confined to the Quaternary arc, a subset of the High Cascades physiographic subprovince.

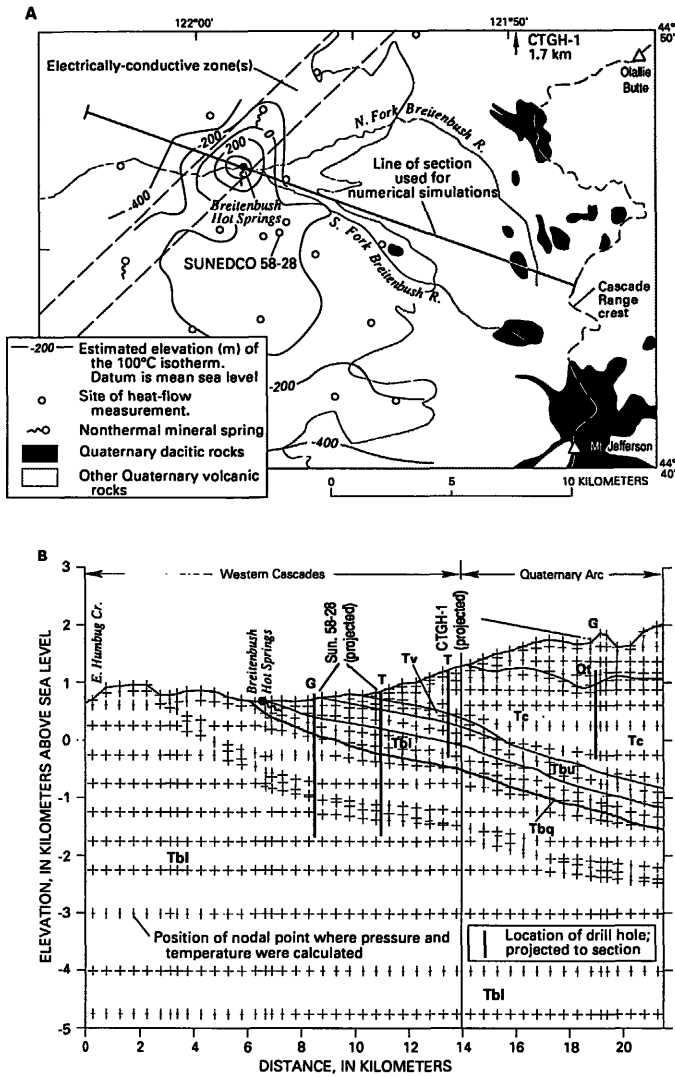


Fig. 2 (a) Map of the Breitenbush Hot Springs area showing the line of section used in numerical simulations, the locations of thermal and nonthermal mineral springs, Quaternary volcanic rocks, electrically-conductive structures identified by H. Pierce and others (written communication, 1989), and the estimated elevation of the 100°C isotherm. Geologic data are from D.R. Sherrod and R.M. Conrey, unpublished mapping. (b) Cross section used for numerical simulation of the Breitenbush Hot Springs system. Lithologic units are described in Table 1. The Sunedco 58-28 and CTGH-1 drill holes, which lie off the section (Figure 2a), are projected to the section in two different ways to indicate their appropriate geologic and topographic contexts. "Geologic" projection (G) locates the drill hole correctly relative to stratigraphic contacts and "topographic" projection (T) puts the collar elevation at the land surface.

NUMERICAL SIMULATIONS

We simulated ground-water flow and heat transport through two generalized cross sections west of the Cascade Range crest: one in the Breitenbush area, where

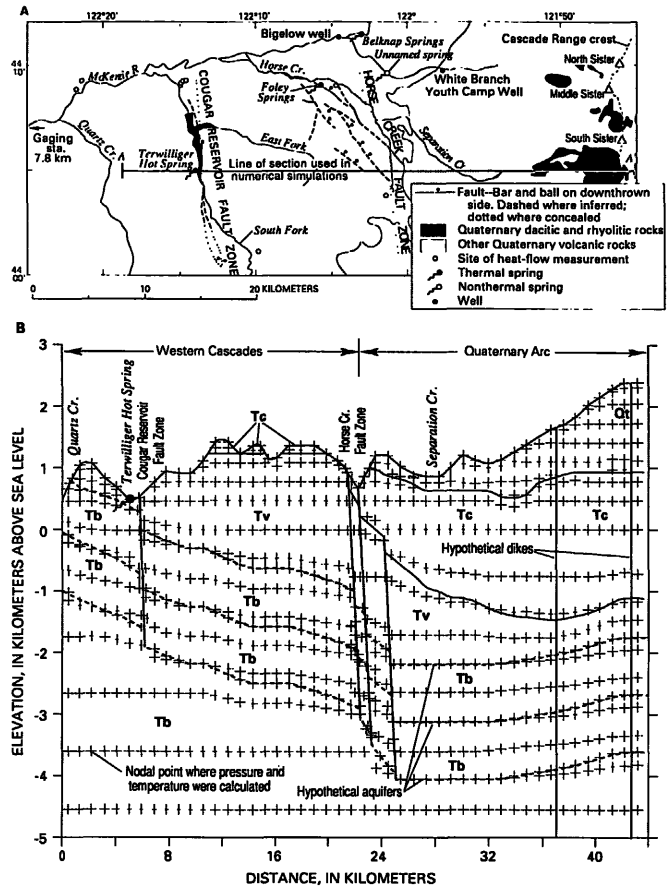


Fig. 3 (a) Map of the McKenzie River area showing the line of section used in numerical simulations, the locations of thermal springs and other selected springs and wells, faults, and Quaternary volcanic rocks. Geologic data are from Priest and others (1988) and from D.R. Sherrod, unpublished compilation map. (b) Cross section used for numerical simulation of the McKenzie River area. Lithologic units are described in Table 1. The hypothetical dikes underly silicic vents near South Sister; zones of relatively high vertical permeability associated with such dikes could enhance deep recharge in the Quaternary arc.

there is no evidence for major arc-parallel normal faulting (Figure 2), and one in the McKenzie River drainage, where major graben-bounding faults exist (Figure 3). We used Bodvarsson's (1982) numerical code PT, which employs an integrated-finite-difference method to solve coupled equations of heat and energy transport. The simulations are only weakly constrained by available data, but allow us to examine some of the thermal and hydrologic implications of the alternate conceptual models depicted in Figure 1.

There is little permeability data available for the study area, but ground-water recharge estimates from stream flow data, conductive heat-flow data (Ingebritsen and others, 1988), and limited well-test data (McFarland, 1982)

Table 1. -- Description of rock units and values of permeability, porosity, and thermal conductivity assigned in numerical simulations

Symbol	Description	Permeability, in m^2	Porosity	Thermal Conductivity, in $W/m \cdot K$
Qt	< 2.3 Ma chiefly lava flows and domes	1.0×10^{-14}	.15	1.55
Tc	4-8 Ma lava flows and minor pyroclastic rocks	5.0×10^{-16}	.10	1.55
Tv	8-17 Ma lava flows (8-13 Ma in Breitenbush area)	1.0×10^{-16}	.05	1.65
Tb	18-25 Ma chiefly volcanic and volcanoclastic strata (divided into Tbu and Tbl in Breitenbush area)	1.0×10^{-17} (Tbu: 5.0×10^{-17})	.05	2.00 (Tbu: 1.50)
Tbq	Quartz-bearing ash-flow tuff in the Breitenbush area (Priest and others, 1987)	2.5×10^{-14}	.02	2.00

suggest that the older rocks are generally less permeable than the younger rocks. Table 1 includes a description of lithologic units and the values of permeability, porosity, and thermal conductivity assigned to those units. The values of porosity and thermal conductivity shown in Table 1 were used in all of the simulations, but permeabilities were varied about the listed values in some cases. The range of permeability values shown in Table 1 is the minimum range required to reproduce the heat-flow observations. Bulk permeabilities $> 10^{-17} m^2$ in the oldest rocks (Table 1: Tb) allow widespread advective transport; this is inconsistent with the heat-flow data, which suggest that significant advective transport in these rocks is only very localized. Permeabilities $< 10^{-14} m^2$ in the youngest rocks (Qt) lead to near-surface heat flow values that are consistently higher than those observed. For the intermediate units, we assumed a rough inverse correlation between permeability and age. The permeability values in Table 1 were used in all simulations unless otherwise noted.

BREITENBUSH SECTION

The 21.5-km-long Breitenbush cross section extends west-northwest from the Cascade Range crest through Breitenbush Hot Springs (Figure 2a). There are a number of 0.025-0.7 Ma dacite domes near the eastern part of the section (Figure 2a), and the underlying silicic magmatic system is a possible heat source for the hydrothermal system (Smith and Shaw, 1975). Temperature-depth data from the Breitenbush area suggest a broad region of

elevated temperatures extending south of Breitenbush Hot Springs. The elevation of the $100^\circ C$ isotherm (Figure 2a) is estimated from the elevation of the hot springs, temperature-depth data from the Sunedco 58-28 drill hole, and projection of terrain-corrected gradients from 15 other drill holes. The Sunedco 58-28 drill hole intercepted a thermal aquifer at ~800 m depth, in or near Priest and others' (1987) map unit Tbq. All of the spring orifices at Breitenbush Hot Springs are at approximately the same stratigraphic level (Priest and others, 1987). This coincidence, and the broad upwarp in the $100^\circ C$ isotherm, suggest the presence of a stratigraphically-controlled aquifer. We treated Tbq as a 30-m-thick zone of relatively high permeability (Figure 2b).

The 6- to 7-km-deep integrated-finite-difference grid shown as Figure 2b was used to simulate ground-water flow and heat transport in the Breitenbush section; pressure and temperature solutions were calculated at 790 nodal points. The lateral boundaries were treated as no-flow (symmetry) boundaries; the lower boundary as a controlled-flux boundary (impermeable to fluid flow, with a specified conductive heat flux); and the upper boundary as a constant pressure-temperature boundary (pressure = 1 bar, temperature = $12.8^\circ C - 5.5^\circ C/km$ above sea level). We simulated the thermal input for the alternate conceptual models depicted in Figure 1 by varying the width and intensity of a basal heat-flow anomaly and, in some cases, by introducing shallow heat sources beneath the Quaternary arc.

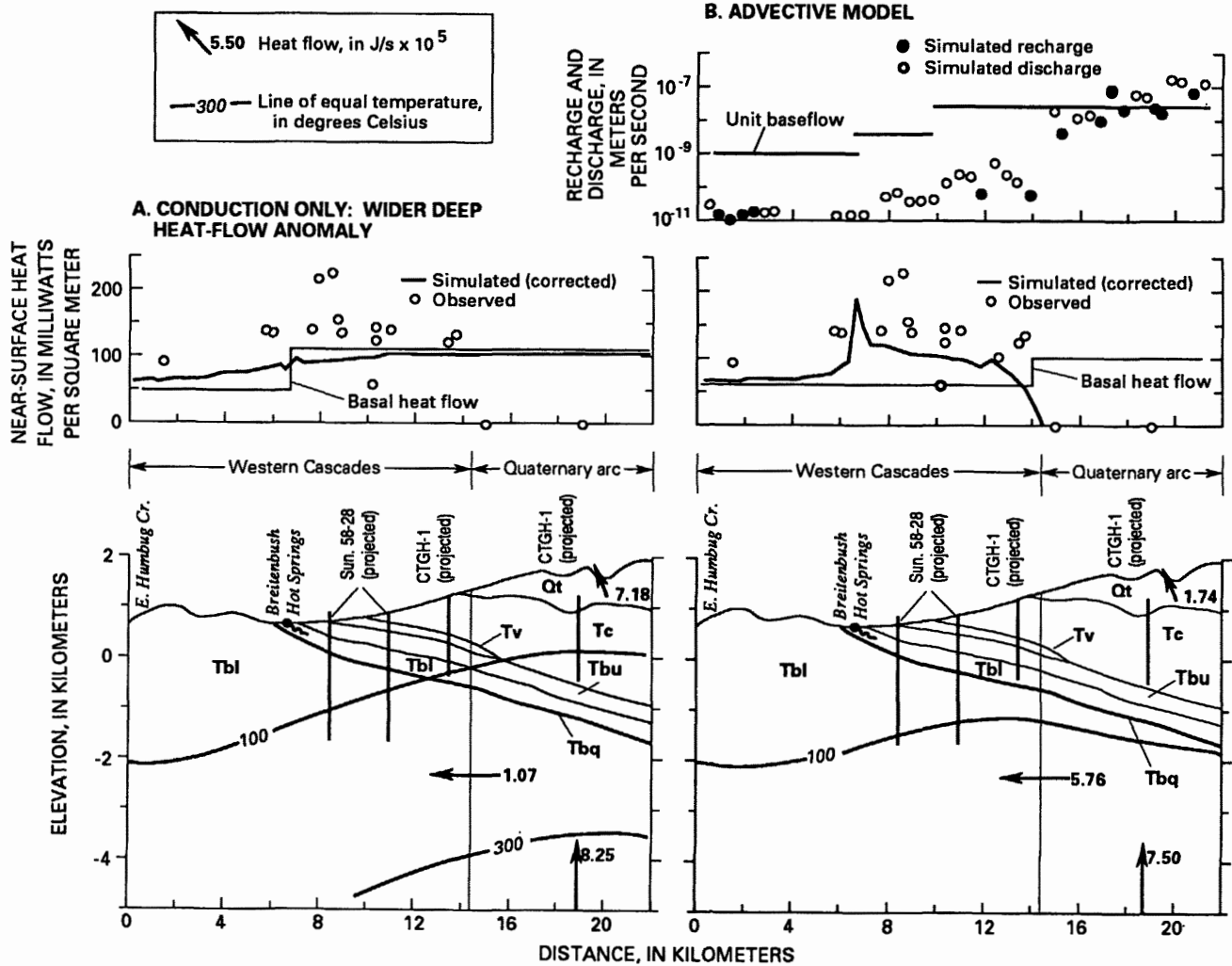


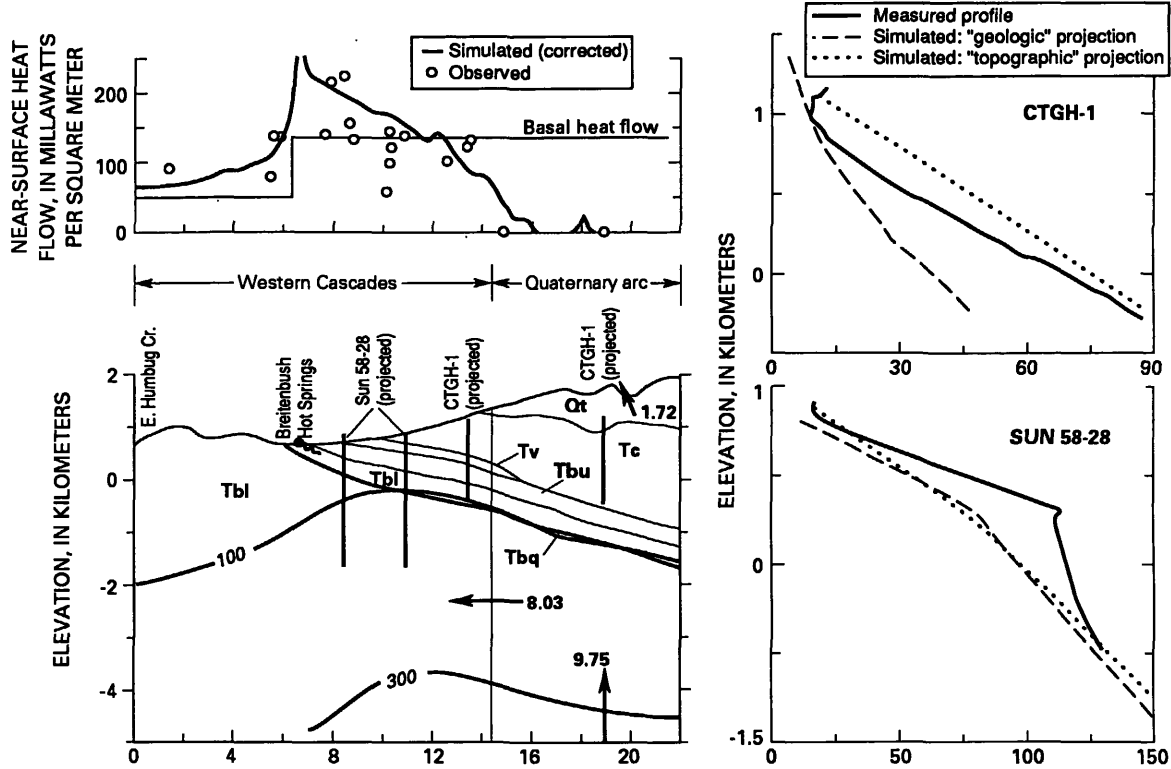
Fig. 4 Selected steady-state results from numerical simulation of the Breitenbush section. Simulated heat-flow values are compared to observed values. In Figure 4b, simulated hydrologic recharge and discharge rates are compared with minimum recharge rates (unit baseflow) that were estimated using stream-flow data from basins where rocks of similar ages are exposed. Labeled arrows indicate how the heat supplied to the Quaternary arc is partitioned. For example, in Figure 4b the basal heat flow totals $7.50 \times 10^5 \text{ J/s}$. Of this quantity, $5.76 \times 10^5 \text{ J/s}$ flow laterally into the Western Cascades and $1.74 \times 10^5 \text{ J/s}$ flow across the land surface within the Quaternary arc.

Figures 4 and 5 show selected steady-state results from numerical simulations of the Breitenbush section. The simulated results are compared with near-surface heat-flow data projected onto the line of section, with ground-water recharge estimates, and, in Figure 5, with temperature profiles from the two deep (>1 km) drill holes in the area, Sunedco 58-28 and CTGH-1 (Figure 2a). Results from a conduction-only simulation with uniform basal heat flow (not shown) were used to make topographic corrections to simulated heat-flow values.

Conduction-only simulations with wide basal heat-flow anomalies (e.g., Figure 4a) failed to reproduce either the low

near-surface conductive heat flows in the High Cascades or the elevated heat flows between Breitenbush Hot Springs and the High Cascades. A simulation with a narrow heat-flow anomaly (Figure 4b) reproduced the observed heat-flow values reasonably well; however, the temperature-depth profiles from the deep drill holes were matched poorly. A conduction-dominated simulation (not shown) with a wide heat source and fluid flow confined to unit Qt matched the data from CTGH-1 fairly well, but failed to reproduce the high heat flows between Breitenbush Hot Springs and the Quaternary arc or the elevated gradient at Sunedco 58-28. If fluid flow is confined to Qt, most of the heat supplied to the Quaternary arc discharges advectively within the arc.

A. ADVECTIVE MODEL, WITH A WIDER, MORE INTENSE DEEP HEAT-FLOW ANOMALY



B. ADVECTIVE MODEL, WITH A LOCALIZED HEAT SOURCE

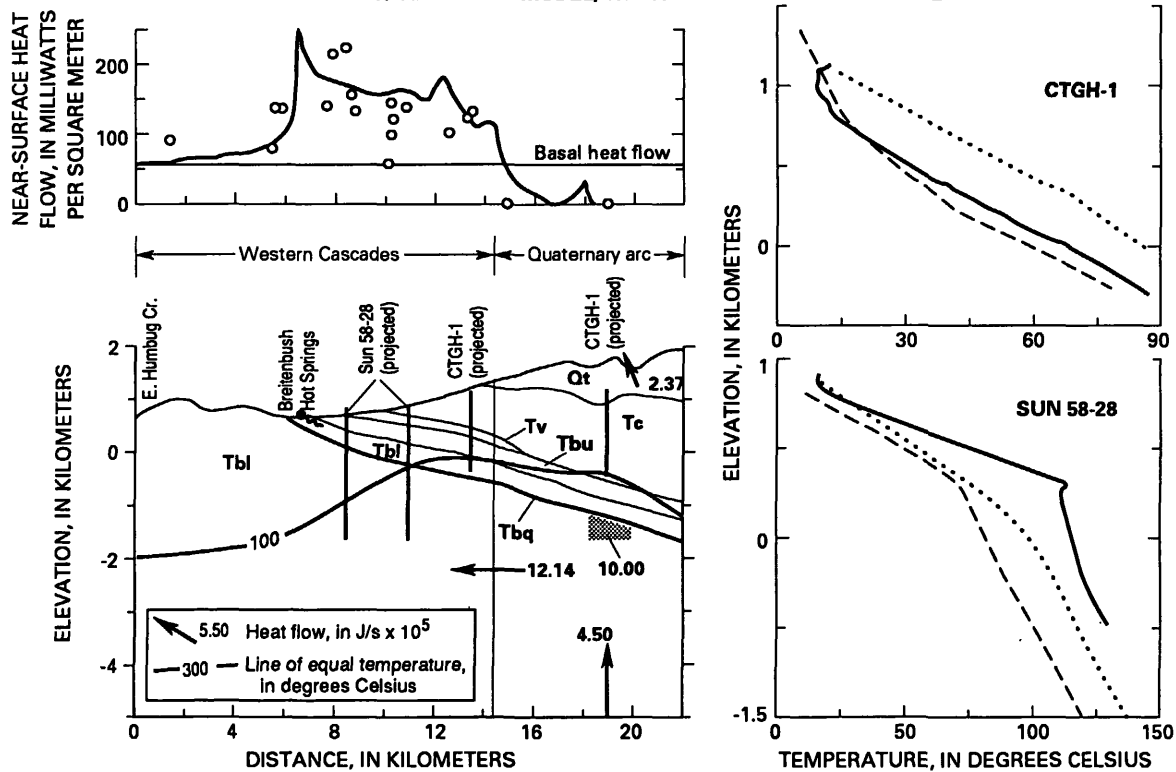


Fig. 5 Selected results from numerical simulation of the Breitenbush section, showing that the thermal observations can be reproduced reasonably well with two very different deep thermal structures. In Figure 5b, the dark polygon in unit Tb1 indicates the location of a heat source producing 10.0×10^5 J/s. The Sunedco 58-28 and CTGH-1 drill holes are off section (Figure 2a) and cannot be projected onto the section in a fashion that reflects both their geologic and topographic contexts. Thus we compare the data from each hole with two simulated temperature profiles, one representing a "geologic" projection and one representing a "topographic" projection (see the caption of Figure 2 for additional information).

Figure 5 shows that both the near-surface heat-flow data and the temperature-depth profiles from the deep drill holes can be reproduced reasonably well with two very different deep thermal structures. The simulation summarized in Figure 5a involved a wide basal heat-flow anomaly of 130 mW/m^2 that is analogous to the mid-crustal heat source model of Figure 1a; the simulation in Figure 5b involved uniform basal heat flux of 60 mW/m^2 and an intense local heat source beneath the Quaternary arc, and is analogous to the lateral-flow model (Figure 1b). Though the heat sources are distributed very differently, the total amount of heat supplied to the system in these two simulations is identical. Both match the observations reasonably well.

Significant advective heat transport is required to reproduce several of the observations from the Breitenbush area, including near-zero near-surface heat flow in the Quaternary arc, elevated heat flow between Breitenbush Hot Springs and the Quaternary arc, and the sharp change in the temperature gradient observed in the Sunedco 58-28 temperature profile. Given significant advective heat transport, the deep thermal structure still cannot be uniquely inferred from the available temperature-depth observations.

MCKENZIE RIVER SECTION

The 43.7-km-long McKenzie River cross section extends west from the Cascade Range crest through Terwilliger Hot Spring (Figure 3a). As is the case in the Breitenbush area, there is silicic volcanism near the eastern part of the section, and the underlying silicic magmatic system(s) may host hydrothermal activity. Silicic volcanic rocks exposed near the eastern end of the section in the South Sister area (Figure 3a) include rhyolites as well as dacites, and are younger than 0.25 Ma.

Temperature-depth data are sparser in the McKenzie River area than in the Breitenbush area, and deep (>1 km) drill-hole data are lacking. In the Breitenbush area, there is suggestive evidence for a zone of relatively high permeability at the approximate stratigraphic horizon of unit Tbq, as explained above. In the McKenzie River area we have experimented with hypothetical 30-m-thick stratigraphically-controlled "aquifers" at three different depths, though there is no direct evidence for such an aquifer unit.

Pressure and temperature solutions for the McKenzie River section were calculated at 921 nodal points within the 5.5- to 7.5-km-deep integrated-finite-difference grid shown as Figure 3b. The

boundary conditions were the same as those used in simulations of the Breitenbush section: the lateral boundaries were no-flow boundaries, the lower boundary a controlled-flux boundary, and the upper boundary a constant pressure-temperature boundary. We again simulate the thermal input for the alternate conceptual models (Figure 1) by varying the distribution of deep heat sources.

We treated the faults (Figure 3b) as 30-m-thick zones of relatively high permeability. The presence of several fault zones and the major topographic divide between Horse Creek and Cougar Reservoir make the McKenzie River section significantly different from the Breitenbush section; the degree of continuity of regional ground-water flow across these barriers is one of the major issues of interest.

Figure 6 shows selected results from numerical simulations of the McKenzie River section. Simulated near-surface heat flow values are compared with data projected onto the line of section, and volumetric flow rates (Darcy velocities) in the hypothetical deep aquifer units are shown for some cases. As was the case with the Breitenbush section, conduction-only simulations with wide basal heat-flow anomalies (e.g., Figure 6a) failed to reproduce the near-surface heat-flow observations satisfactorily. However, the heat-flow data are concentrated near the Horse Creek and Cougar Reservoir fault zones. The elevated heat flow in those areas could be explained in terms of convective circulation within the fault zones themselves, with insignificant advective heat transport in the two dimensions that we simulated.

Figure 6b summarizes the results of three simulations in which the depth to a hypothetical deep aquifer was varied. The 30-m-thick faults and the "aquifer" were assigned permeabilities of $2.5 \times 10^{-14} \text{ m}^2$. These simulations resulted in pronounced conductive heat-flow anomalies at the Horse Creek and Cougar Reservoir fault zones and in the Separation Creek area, but very low heat flow between the two fault zones. In each of these simulations advective heat transfer between the Quaternary arc and the Western Cascades is small, amounting to less than 10 percent of the heat supplied to the Quaternary arc; most of the heat supplied to the Quaternary arc discharges in the Separation Creek area or at the Horse Creek fault zone. Only for the deepest aquifer configuration is there continuous regional ground-water flow and a net transfer of heat from the Quaternary arc to the Western Cascades (see the volumetric flow rates and labeled arrows in Figure 6b).

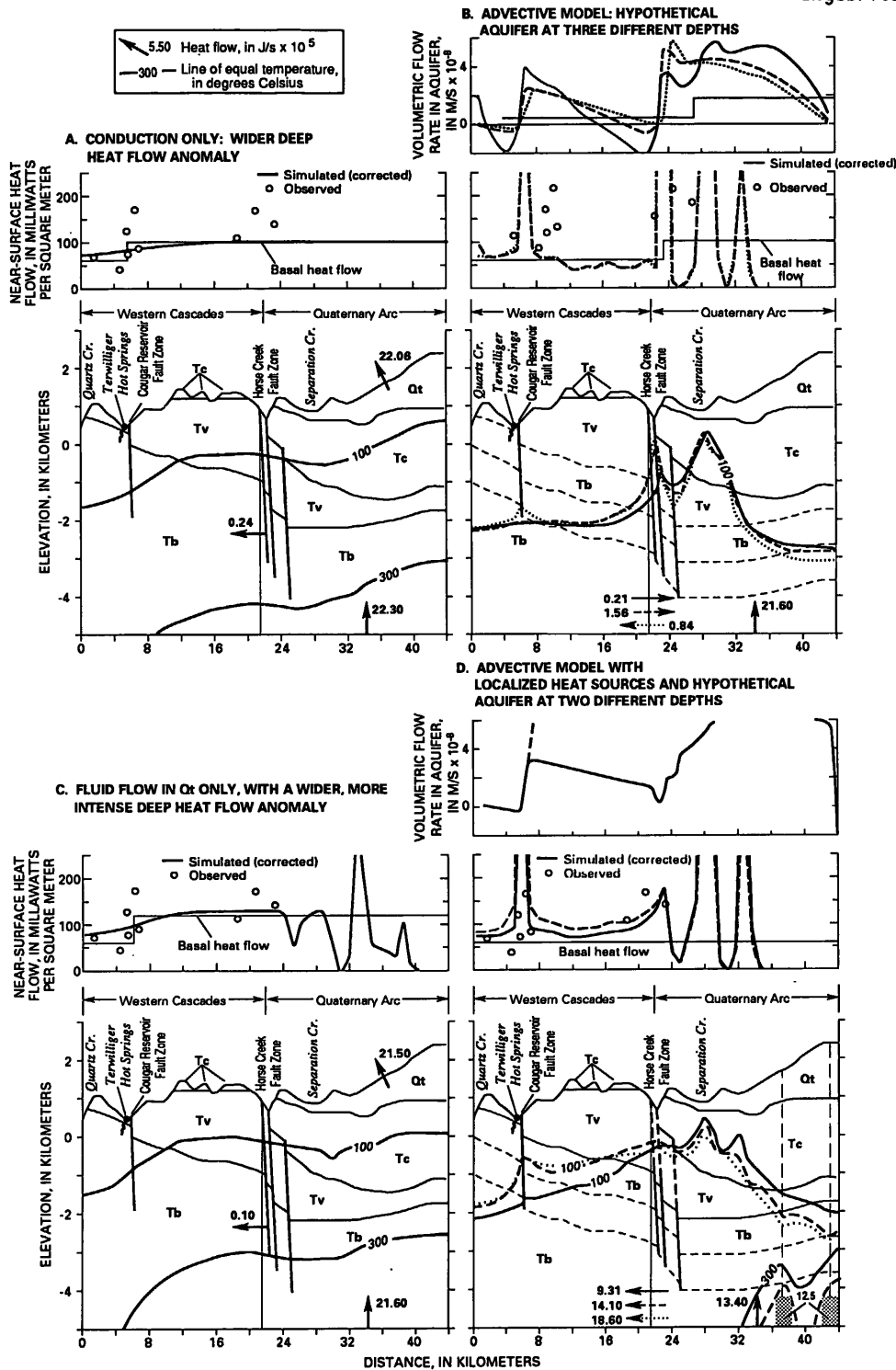


Fig. 6 Selected results from numerical simulation of the McKenzie River section. Simulated heat-flow values are compared to measured values, and simulated volumetric flow rates (Darcy velocities) in the deep "aquifer" unit are shown where applicable. Labeled arrows indicate how the heat supplied to the Quaternary arc is partitioned. In Figure 6b, the solid, dashed, and dotted lines and arrows indicate results for the shallowest, intermediate, and deepest "aquifer" configurations, respectively. In Figure 6d, the solid and dashed lines and arrows indicate results for the shallower and deeper "aquifer" configurations, respectively, and the dotted lines and arrow indicate results from a simulation in which both aquifers were present. The labeled dark rectangles in Figure 6d indicate localized heat sources, each producing $12.5 \times 10^5 J/s$. In the simulations summarized in Figures 6c and 6d the total heat input to the system was identical.

Simulated heat transfer between the Quaternary arc and the Western Cascades is sensitive to the permeability structure. Figure 6d summarizes results from simulations in which the permeability of the upper (dashed) part of the Horse Creek fault zone was reduced to values similar to those assigned to the surrounding rocks; the permeability of unit Tv was lowered to $2 \times 10^{-17} \text{ m}^2$; and two $30 \times 10^{-14} \text{ m}^2$ thick high-permeability vertical conduits were added to enhance deep recharge within the Quaternary arc. These relatively minor modifications to the poorly-constrained permeability structure led to significant net heat transfer; in these simulations, up to ~50 percent of the heat supplied to the Quaternary arc is transferred advectively to the Western Cascades.

As with the Breitenbush section, simulations involving very different distributions of deep heat sources can produce similar matches to the available data. However, unlike the Breitenbush simulations, one of the matches that we consider reasonable for the McKenzie River section is conduction-dominated. A conduction-dominated simulation with a wide basal heat-flow anomaly and fluid flow confined to Qt (Figure 6c) is analogous to the mid-crustal heat source model (Figure 1a) and provides a reasonable match; the elevated heat flows near Horse Creek and Cougar Reservoir fault zones can be explained in terms of circulation in a third (unsimulated) dimension, as noted above.

Simulations involving more localized heat sources (e.g., Figure 6d) are analogous to the lateral-flow model (Figure 1b) and can also match the thermal data reasonably well. Advection-dominated models lead to elevated heat flows between the Horse Creek and Cougar Reservoir fault zones only if there is a zone of relatively high permeability at depths of several kilometers. At shallower depths, regional ground-water flow may be interrupted by the Horse Creek fault zone and the topographic divide between the fault zones.

DISCUSSION

We regard the results presented here as preliminary, pending additional experiments to test their sensitivity to changes in permeability and other properties. The relatively shallow thermal observations do not allow us to distinguish clearly between the two conceptual models. In the future, relevant geochemical data will be used to further constrain the numerical simulations. Deep drilling (3-4 km depth) in areas of high heat flow in the Western Cascades would be the most conclusive test of the alternate models.

ACKNOWLEDGMENTS

D.R. Sherrod drew the cross sections that provided a framework for our integrated-finite-difference grids. Sherrod, H.I. Essaid, T.E.C. Keith, and M.L. Sorey provided helpful technical reviews. David Jones drafted the figures.

REFERENCES CITED

- Blackwell, D.D., and Baker, S.L., 1988, Thermal analysis of the Breitenbush geothermal system: Geothermal Resources Council Transactions, v. 12, p. 221-227.
- Blackwell, D.D., Bowen, R.G., Hull, D.A., Riccio, J., and Steele, J.L., 1982, Heat flow, arc volcanism, and subduction in northern Oregon: Journal of Geophysical Research, v. 87, p. 8735-8754.
- Blackwell, D.D., and Steele, 1985, Heat flow of the Cascade Range in Guffanti, M., and Muffler, L.J.P., eds., Proceedings of the workshop on geothermal resources of the Cascade Range, U.S. Geological Survey Open-File Report 85-521, p. 20-23.
- Blackwell, D.D., Steele, J.L., Frohme, M.K., Murphy, C.F., Priest, G.R., and Black, G.L., 1989, Heat flow in the Oregon Cascade Range and its correlation with regional gravity, magnetic, and geologic patterns in Muffler, L.J.P., Weaver, C.S., and Blackwell, D.D., eds., Proceedings of workshop XLIV: Geological, geophysical, and tectonic setting of the Cascade Range: U.S. Geological Survey Open-File Report 89-178, p. 142-170.
- Bodvarsson, G.S., 1982, Mathematical modeling of geothermal systems: Ph.D. thesis, University of California, Berkeley, 348 p.
- Ingebritsen, S.E., Mariner, R.H., Cassidy, D.E., Shepherd, L.D., Presser, T.S., Pringle, M.K.W., and White, L.D., 1988, Heat-flow and water-chemistry data from the Cascade Range and adjacent areas in north-central Oregon: U.S. Geological Survey Open-File Report 88-702, 205 p.
- Ingebritsen, S.E., Sherrod, D.R., and Mariner, R.H., 1989, Heat flow and hydrothermal circulation in the Cascade Range, north-central Oregon: Science, v. 243, p. 1,458-1,462.
- McFarland, W.D., 1982, A description of aquifer units in western Oregon: U.S. Geological Survey Open-File Report 82-165, 35 p.
- Priest, G.R., Black, G.L., and Woller, N.M., 1988, Geologic map of the McKenzie Bridge quadrangle, Lane County, Oregon: Oregon Department of Geology and Mineral Industries Geological Map Series GMS-48, map scale 1:62,500.
- Priest, G.R., Woller, N.M., and Ferns, M.L., 1987, Geologic map of the Breitenbush River area, Linn and Marion Counties, Oregon: Oregon Department of Geology and Mineral Industries Geological Map Series GMS-46, map scale 1:62,500.
- Smith, R.L., and Shaw, H.R., 1975, Igneous-related geothermal systems in White, D.E., and Williams, D.L., eds., Assessment of geothermal resources of the United States - 1975: U.S. Geological Survey Circular 726, p. 58-83.